Hydrol. Earth Syst. Sci. Discuss., 9, 12691–12727, 2012
www.hydrol-earth-syst-sci-discuss.net/9/12691/2012/
doi:10.5194/hessd-9-12691-2012

Hydrology and Earth System Sciences Discussions

This discussion paper is/has been under review for the journal Hydrology and Earth System Sciences (HESS). Please refer to the corresponding final paper in HESS if available.

New climate change scenarios reveal uncertain future for Central Asian glaciers

A. F. Lutz[1,2], W. W. Immerzeel[1,2,3], A. Gobiet[4], F. Pellicciotti[3], and M. F. P. Bierkens[2,5]

[1]FutureWater, Wageningen, The Netherlands
[2]Department of Physical Geography, Utrecht University, Utrecht, The Netherlands
[3]Institute of Environmental Engineering, Hydrology and Water Resources Management, ETH Zurich, Zurich, Switzerland
[4]Wegener Center for Climate and Global Change, University of Graz, Graz, Austria
[5]Deltares, Utrecht, The Netherlands

Received: 25 October 2012 – Accepted: 30 October 2012 – Published: 8 November 2012

Correspondence to: A. F. Lutz (a.lutz@futurewater.nl)

Published by Copernicus Publications on behalf of the European Geosciences Union.

Abstract

Central Asian water resources largely depend on (glacier) melt water generated in the Pamir and Tien Shan mountain ranges, located in the basins of the Amu and Syr Darya rivers, important life lines in Central Asia and the prominent water source of the Aral Sea. To estimate future water availability in the region, it is thus necessary to project the future glacier extent and volume in the Amu and Syr Darya river basins. The aim of this study is to quantify the impact of uncertainty in climate change projections on the future glacier extent in the Amu and Syr Darya river basins. The latest climate change projections provided by the fifth Coupled Model Intercomparison Project (CMIP5) generated for the upcoming fifth assessment report of the Intergovernmental Panel on Climate Change (IPCC) are used to model future glacier extent in the Central Asian region for the two large river basins. The outcomes are compared to model results obtained with the climate change projections used for the fourth IPCC assessment (CMIP3). We use a regionalized glacier mass balance model to estimate changes in glacier extent as a function of glacier size and projections of temperature and precipitation. The model is developed for implementation in (large scale) hydrological models, when the spatial model resolution does not allow for modelling of individual glaciers and data scarcity is an issue. Both CMIP3 and CMIP5 model simulations point towards a strong decline in glacier extent in Central Asia. However, compared to the CMIP3 projections, the CMIP5 projections of future glacier extent in Central Asia provide a wider range of outcomes, mostly owing to greater variability in precipitation projections among the latest suite of climate models. These findings have great impact on projections of the timing and quantity of water availability in glacier melt dominated rivers in the region. Uncertainty about the size of the decline in glacier extent remains large, making estimates of future Central Asian glacier extent and downstream water availability uncertain.

1 Introduction

The fate of Asian glaciers under climate change has been the topic of a heated scientific and societal debate (Bolch et al., 2012; Cogley et al., 2010; Immerzeel et al., 2010; Kargel et al., 2011; Sorg et al., 2012). The underlying reason of this ongoing debate is the lack of systematic cryospheric observations and the absence of robust methods that can assess glacier evolution under climate change at the large river basin scale. Future glacier extent is a combined result of glacier mass balance (i.e. net mass loss or gain) and ice-flow dynamics of glaciers. Both processes can be modelled with a variety of approaches of different complexity, but for large scale simulations and data scarce areas simple models need to be used (Radić and Hock, 2011). These models are commonly forced by air temperature and precipitation provided by General Circulation Models (GCMs) which are downscaled to the study region. However, there is large spread in the GCM projections (Radić and Clarke, 2011), and this is especially true for precipitation in Asia (Immerzeel et al., 2010). There is growing agreement in the scientific community that impact studies should be forced by an ensemble of GCMs outputs. While this has been done for the North-American (Radić and Clarke, 2011), European region (Huss, 2011) or for selected glaciers (e.g. Giesen and Oerlemans, 2010), no such assessments are available for Central Asia.

The aim of this study is to quantify the impact of uncertainty in climate change projections on the future glacier extent in the Amu Darya and Syr Darya river basins in Central Asia; two melt-water dominated rivers which provide the most important water sources in the Central Asian region. To achieve this, a glacier model is developed to simulate the future response of glaciers and changes in glacier geometry at the large-scale, under data scarce conditions. This model is forced with precipitation and temperature projections from 2001 to 2050 based on a comprehensive assessment of the CMIP3 and the new CMIP5 multi-model ensembles. We quantify the uncertainty in glacier projections as a result of uncertainty in the climate forcing and we show how this uncertainty differs between CMIP3 and CMIP5.

HESSD
9, 12691–12727, 2012

2 Study area

The Amu Darya and Syr Darya rivers traverse a geopolitically complex region. Their sources are located in the Pamir and Tien Shan mountains respectively (Fig. 1), and both rivers eventually drain into the Aral Sea. Water allocation is a highly sensitive topic in the region. The upstream countries Kyrgyzstan and Tajikistan use water mainly for hydropower production during winter whereas the downstream countries (Uzbekistan, Turkmenistan and Kazakhstan) utilize water for irrigation during summer where around 22 million people depend on irrigated agriculture (Siegfried et al., 2012). Glacial melt provides an important source of water in both basins, given the dry and warm climate downstream (Kaser et al., 2010; Sorg et al., 2012). The present total glacierized area in the Amu Darya basin is 16 451 km^2 (2.1 % of total basin area) and 1738 km^2 (0.16 % of total basin area) in the Syr Darya basin (Raup et al., 2007). Significant reductions in area and volume have been reported for the Tien Shan (Aizen et al., 2007a,b; Bolch, 2007; Khromova et al., 2003; Narama et al., 2010; Siegfried et al., 2012) and Pamir mountains (Khromova et al., 2006) during the last decades.

3 Data

For this study digital elevation models (DEMs), meteorological station data, climate change projections produced with GCMs and data on glaciers are used to estimate future glacier extent in the Central Asian region.

3.1 Digital elevation models

In this study two DEMs are used. Both are based on the Shuttle Radar Topographic Mission (SRTM) DEM at a nominal resolution of 90 m. For the downscaling of GCMs, this DEM is resampled to 1 km resolution. This DEM is further referred to as the 1 km DEM. This is the spatial resolution of the glacier model. However, for sub-grid

HESSD
9, 12691–12727, 2012

calculations, the SRTM DEM at high resolution (90 m) is used. This DEM is further referred to as the 90 m DEM.

3.2 Climate reference period

A climatic dataset of ten years (2001–2010) of high spatial and temporal resolution is used as reference for the climate change assessment. For this period, we use the PERSIANN dataset for precipitation and ground station data for temperature. Daily precipitation data are bilinearly interpolated to 1 km resolution from the PERSIANN 0.25° neural network based precipitation dataset (Hsu and Sorooshian, 2009). A quality check was performed on the PERSIANN time series using station observations and unrealistic outliers were replaced by data from the TRMM dataset (Kaushik et al., 2010). Gridded daily average near-surface air temperature data at 1 km resolution are obtained by interpolation of station data. Daily temperature observations from 124 stations spread over the upstream and downstream areas in the Amu Darya and Syr Darya basins are interpolated by universal kriging to 1 km spatial resolution and subsequently corrected for elevation using the 1 km DEM and a vertical temperature lapse rate (Table 1). Of these 124 stations, thirty are located within the boundaries of the studied upstream parts of the basins (Fig. 1). All station observations used were extracted from the GOSIC dataset (http://gosic.org).

3.3 Climate change projections

We use the latest set of global climate change simulations, the CMIP5 multi-model ensemble (Taylor et al., 2012) which is also used as basis for the upcoming fifth assessment report of the Intergovernmental Panel on Climate Change (IPCC). All simulations which were available online in the PCMDI database (http://cmip-pcmdi.llnl.gov/cmip5/) earlier than 15 December 2011 are included in the analysis. In order to compare the CMIP5 multi-model ensemble to the recent generation of global climate change

HESSD
9, 12691–12727, 2012
Uncertain future Central Asian glaciers
A. F. Lutz et al.

simulations, the CMIP3 multi-model ensemble (Meehl et al., 2007), which is the basis of the current fourth IPCC assessment report is also analysed.

We consider the CMIP3 and CMIP5 simulations based on all available emission scenarios: SRES B1, A1B, and A2 (Nakicenovic et al., 2000) in the case of CMIP3 and rcp2.6, rcp4.5, rcp6.0, and rcp8.5 (Meinshausen et al., 2011) in the case of CMIP5. Since it is difficult to associate probabilities to the emission scenarios, we do not use any prior assumption and give the same weight to all scenarios, thus sampling all scenarios and GCM runs with equal inclusion probabilities. This is realized by calculating weighted percentiles according to the inverse number of simulations per scenario. We analyse projected annual temperature and precipitation averaged over the period 2021–2050 and compare it to the period 1961–1990. Hence, the climate change signals refer to change during 60 years.

Both the CMIP3 and CMIP5 ensembles show large variation in temperature and precipitation changes between models and between emission scenarios (Figs. 2, 3). On average, temperature is expected to rise by about 2 °C and precipitation to remain nearly constant. The uncertainty in temperature projections (ΔT), expressed as the 90th and 10th percentiles, is estimated to range from 1.3 °C to 2.4 °C in the CMIP3 ensemble and from 1.7 °C to 2.9 °C in the CMIP5 ensemble (Fig. 3, left panel). For precipitation projections (ΔP) it ranges from −6 % to +7 % in the CMIP3 ensemble and from −8 % to +15 % in the CMIP5 ensemble (Fig. 3, right panel). Though the climate projections of both ensembles mainly cluster around the same values (about 2 °C and 0 %), the new CMIP5 ensemble includes the possibility of more extreme climate change. There are several "warmer" simulations (up to +3.5 °C) and many of those are also extreme in precipitation change (Fig. 2). Note that this observation not only holds across scenarios, but also between GCM runs within a given scenario. e.g. RCP 2.6, 6.0 and 8.5 show similar extremes in temperature and precipitation. The CMIP5 ensemble also shows a larger average warming than CMIP3 (Fig. 3, left panel), which is a result of the skewed temperature change distribution with its heavy tail on the warm

HESSD
9, 12691–12727, 2012

Uncertain future Central Asian glaciers

A. F. Lutz et al.

side (Fig. 2). In addition, the variation between scenarios is also larger for CMIP5 for both precipitation and temperature (Fig. 3).

3.4 Glaciers

Glacier covered areas in the Pamir and Tien Shan mountain ranges in the Amu and Syr Darya river basins are extracted from the GLIMS dataset (Raup et al., 2007), recently updated for the Central Asian region (see acknowledgements). The GLIMS dataset does not completely cover the entire study area and is complemented with glacier boundaries from the digital chart of the world (Danko, 1992). We assume this compiled dataset of glacier extent to represent the glacier extent at the end of the reference period, as starting point for the future simulations of glacier extent.

From this dataset with glacier extents, the size distribution of glaciers is extracted. Fig. 4 shows the distribution of glacier sizes. In the Amu Darya and Syr Darya river basin, 80 % of the total glacier area consists of glaciers with a surface area smaller than 25 km^2 and 16 % of all glaciers is smaller than 1 km^2. The median glacier size in the basin is 5.0 km^2. From this distribution 21 different glacier size classes are defined and used for further analysis (Fig. 4).

The initial fractional glacier cover per 1 km grid cell is also extracted from the dataset with glacier extents, to be used as starting point in the glacier model simulation. Each 1 km grid cell from the 1 km DEM is assigned a fractional glacier cover varying from 0 (no glacier cover) to 1 (entirely covered with glaciers) (Fig. 1).

The observed average annual mass balance in the region's mountains is approximately −0.44 m water equivalent (w.e.) between 2001 and 2010, based on several bench mark glaciers in the region (WGMS, 2011) (Table 2).

4 Methods

4.1 Downscaling of GCM output

Downscaling of the GCMs outputs is necessary due to the large scale discrepancy between the climate models (operated on grids of 100 km grid distance or more) and the glacier model (operating on the 1 km scale). In our study, the major focus is on uncertainty stemming from the climate simulations, so we include as many climate simulations as possible. We extract the grid cells of the climate models over the study region to calculate climate change signals (2012–2050 compared to 1961–1990). We derive the 10th(Q10), 25th(Q25), 50th(Q50), 75th(Q75) and 90th(Q90) percentile values of the changes in precipitation and temperature for the entire CMIP3 and CMIP5 ensemble. We compute a "delta change" value for each percentile and year assuming a constant rate of change. We repeat the reference period (Sect. 3.2) four times and we superimpose the annual temperature and precipitation change values to construct a transient time series from 2011 to 2050. These time series are then used as meteorological forcing for the glacier model, which is run with all the combinations of the percentile values of changes in precipitation and temperature. This well established "delta change" approach (Arnell, 1999; Kay et al., 2008) removes large parts of climate model's biases, which cancel out in the climate change signals. However, changes in inter-annual variability and annual cycle are neglected, since these climate characteristics are inherited from the observations (Deque, 2007).

4.2 Glacier model

The glacier model used in this study is a newly developed approach with minimum data requirements. It is a mass balance model with parameterization of glacier geometry changes and subsequent aggregation of regional glacier characteristics. The model estimates the fractional glacier coverage (F_G) for each 1 km grid cell at a monthly time step, as a function of the glacier size and temperature and precipitation projections.

HESSD
9, 12691–12727, 2012
Uncertain future Central Asian glaciers
A. F. Lutz et al.

The glacier model requires daily temperature and precipitation, elevation data and the initial glacier fraction for each 1 km grid cell (Sect. 3). Figure 5 provides a schematic representation of the modelling steps described below.

4.2.1 Basin scale hypsometric curve

To setup the glacier model for the studied basins, we construct a basin scale hypsometric curve. Therefore we need to derive the median glacier elevation (H_{GLAC}) in a 1 km grid cell. First we use the 90 m DEM to calculate the average elevation (H_{AVG}) and standard deviation of the elevation (H_{SD}) within each 1 km grid cell. We then derive the median glacier elevation in a 1 km grid cell (H_{GLAC}) based on the distribution of elevation and F_{G}, assuming that within a 1 km grid cell the glacier distribution is proportional to the elevation distribution and glaciers occupy the highest (coldest) end of the elevation distribution.

Figure 6 shows schematically how H_{GLAC} can be determined from H_{AVG} and H_{SD}. It shows the elevation distribution within a 1 km grid cell and the elevations occupied by the glacier. If we assume the elevation distribution to be approximately normal, then we can estimate the median glacier elevation as:

$$H_{\mathrm{GLAC}} = H_{\mathrm{AVG}} + H_{\mathrm{SD}} \cdot F_N^{-1}\left(1 - \frac{F_{\mathrm{G}}}{2}\right) \tag{1}$$

where $F_N^{-1}\left(1 - \frac{F_{\mathrm{G}}}{2}\right)$ is the $1 - \frac{F_{\mathrm{G}}}{2}$ quantile of the standard normal distribution. We combine these data for all grid cells to derive a basin scale hypsometric curve (Fig. 7), representative for the average glacier in the region of interest.

4.2.2 Mass balance per glacier size class

For each glacier size class (Sect. 3.4) separately, we calculate a basin scale monthly glacier mass balance. The representative air temperature for the mean elevation of the

HESSD
9, 12691–12727, 2012

glacierized fraction of a 1 km grid cell (T_{GLAC}) is defined as:

$$T_{GLAC} = T_{AVG} + (H_{GLAC} - H_{AVG}) \cdot T_{lapse} \quad (2)$$

where T_{AVG} is the air temperature at H_{AVG} (°C) and T_{lapse} is a temperature lapse rate (°C m^{-1}) (Table 1). We average T_{GLAC} for all (partly) glacierized grid cells to obtain a monthly temperature, representative for the entire glacierized area in the two basins:

$$\overline{T}_{GLAC} = \frac{1}{n} \sum_{i=1}^{n} T_{GLAC} \quad (3)$$

where n is the number of (partly) glacierized grid cells.

In the same way, we average H_{GLAC} for all (partly) glacierized grid cells to obtain one value for H_{GLAC}, representative for the entire glacierized area in the two basins:

$$\overline{H}_{GLAC} = \frac{1}{n} \sum_{i=1}^{n} H_{GLAC} \quad (4)$$

where n is the number of (partly) glacierized grid cells.

For each month we derive the basin-scale altitude of the 0 °C isotherm (H_0), using $\overline{H}_{GLAC}$, $\overline{T}_{GLAC}$ and the same temperature lapse rate (Table 1):

$$H_0 = \overline{H}_{GLAC} + \overline{T}_{GLAC} \cdot T_{lapse}^{-1} \quad (5)$$

We use the 0 °C isotherm altitude in combination with the hypsometric curve to estimate the monthly accumulation area ratio (AAR) at basin-scale, defined as the accumulation area divided by the total area. We then determine the median elevation for the ablation zone (H_{ABL}) and accumulation zone (H_{ACC}) at basin-scale using the hypsometric curve and the AAR. Using the AAR, both the ablation area and accumulation area are updated every month, for each glacier size class separately. The following steps are thus performed for each glacier size class separately.

HESSD
9, 12691–12727, 2012

Title Page
Abstract Introduction
Conclusions References
Tables Figures
◀ ▶
Back Close
Full Screen / Esc
Printer-friendly Version
Interactive Discussion

We approximate the average temperature for the ablation zone (T_{ABL}) by lapsing T_{GLAC} to H_{ABL} using a temperature lapse rate (Table 1). The monthly ablation (A_m [m^3]) is calculated as:

$$A_m = T_{ABL} \cdot DDF \cdot d_m \cdot S_a \tag{6}$$

where DDF is a composite degree day factor (mm °C^{-1}day^{-1}, Table 1) that includes the relative proportion of debris free glaciers (85 %) and debris covered glaciers (15 %) for glacier melt, d_m is the number of days in the month with average temperature above 0 °C, and S_a is the ablation area (m^2). The DDF for debris free and debris covered glaciers were calibrated for a related hydrological study (Immerzeel et al., 2012a). These values are within the range of other studies reported in the region (Hagg et al., 2008; Immerzeel et al., 2010, 2012b; Mihalcea et al., 2006; Zhang et al., 2006). In addition we take into account variation in DDF in the uncertainty analysis described in Sect. 4.3. The monthly accumulation (C_m [m^3]) is calculated as:

$$C_m = P_m \cdot S_c \tag{7}$$

where P_m is the monthly precipitation (m) and S_c is the accumulation area (m^2). All precipitation over the accumulation zone is assumed to be solid. An initial ice volume is determined using the following relation between volume and area (Bahr et al., 1997).

$$V = 0.12 \cdot A^{1.375} \tag{8}$$

where V is the ice volume (m^3) and A is the glacier area (m^2). We use the monthly melt and accumulation to update the ice volume each month and using the inverse of Eq. (8) we determine a new glacier area, being the starting point for the next month's calculations. We repeat the calculations for each month in the reference period and for all glacier size classes. Each month a specific mass balance (m w.e. y^{-1}) is determined.

HESSD
9, 12691–12727, 2012
Uncertain future Central Asian glaciers
A. F. Lutz et al.

4.2.3 Calibration

Based on the observed mass balance in the region (Sect. 3.4, Table 2) the glacier model is calibrated by correcting the monthly mean temperature between 2001 and 2010 with a temperature correction (CorT) (Table 1). With the calibrated CorT, the model produces the same mass balance for the reference period as the average observed mass balance in the basins. The CorT parameter accounts for a combined effect of temperature differences within a 1 km grid cell, vertical and horizontal interpolation errors in the reference period climate dataset and errors from averaging over the two basins. Besides, it corrects for the significant error in the precipitation data used that is especially large over mountain areas. After calibration the simulated average annual AAR over the 2001–2010 period was determined (AAR = 0.665) and this matches well with earlier reported values based on inventory data from over 24,000 Eurasian glaciers (annual AAR = 0.578) (Bahr et al., 1997).

4.2.4 Simulating future glacier extent

To simulate future glacier extent in the Amu and Syr Darya river basins, we force the calibrated model with the downscaled future temperature and precipitation projections described in Sect. 4.1. By aggregating the results for all size classes, the change in glacier area from 2011 to 2050 is determined and an area depletion curve is constructed (Table 2).

To produce maps of projected fractional glacier cover per grid cell we downscale the basin-average results from the glacier model to 1 km. We combine the area depletion curve and the hypsometric curve to determine the threshold elevation below which glaciers do not persist (H_{GT}) for each month from 2011–2050 (Table 2).

We update the fractional glacier cover for each grid cell for each month using H_{GT} and the elevation distribution within a 1 km grid cell. Again assuming that the glacier distribution is proportional to the distribution of elevation and the latter can be described by normal distribution, we calculate F_G for a 1 km grid cell using the following

HESSD
9, 12691–12727, 2012

parameterized version of the cumulative standard normal curve function:

$$F_\mathrm{G} = 1 - \left(\frac{1}{2} + \frac{\arctan(z \cdot (c1 + c2 \cdot z^2))}{\pi}\right) \tag{9}$$

where

$$z = \frac{H_\mathrm{GT} - H_\mathrm{AVG}}{H_\mathrm{SD}} \tag{10}$$

Fig. 9 shows how a larger variation of elevation within a 1 × 1 km grid cell leads to a more gradual simulated decrease in fractional glacier coverage.

4.2.5 Model sensitivity

We analyse the model sensitivity by forcing it with hypothetical scenarios for precipitation, temperature, size and melt rate (Fig. 10). Our analysis shows that for a 5 km^2 glacier in this region a 20 % increase in average annual precipitation compensates the effect of a 1 °C temperature increase (panel A and B).

The non-linear volume-area scaling properties of glaciers also have a large influence on glacier changes (Bahr et al., 1997). In the Pamir and Tien Shan the majority of glaciers has an area less than 1 km^2, however a relative small number of large glaciers, such as the Fedchenko glacier system in the Pamir mountains, contain substantial parts of the ice volume of the basin. These large glaciers retreat much slower than small glaciers because of their smaller area-to-volume ratio, e.g. a glacier of size 1 km^2 has completely disappeared by 2026, whereas for a glacier of 100 km^2 89 % of its original area remains (panel C).

Panel D shows that the model is highly sensitive to the DDF. Glacier albedo and surface properties largely determine variability in melt rates. For example, debris cover on glacier tongues has a strong insulating effect, whereas a thin layer of deposited black carbon may increase melt rates significantly (Hagg et al., 2008; Menon et al., 2010).

HESSD
9, 12691–12727, 2012

4.3 Uncertainty analysis

The glacier model is subject to uncertainties in the model parameters as well as uncertainty in the observed historical glacier mass balance used to constrain the parameters. We quantify how these uncertainties translate in uncertainty in the future glacier extent by running the model for different sets of parameters and observed glacier mass balance. We assume the three critical model parameters (T_{lapse}, DDF_{CI}, DDF_{DC}) to be three independent Gaussian deviates. We use a mean DDF_{DC} = 3.97 mm °C^{-1} d^{-1} and DDF_{CI} = 7.95 °C^{-1} d^{-1} and both with σ = 1°C^{-1} d^{-1}). These degree day factors were calibrated in a related hydrological study in the Amu Darya and Syr Darya river basins (Immerzeel et al., 2012a). For T_{lapse} we use a mean −0.0068 °C m^{-1} and assume a standard deviation of 0.0012°C m^{-1}, which is based on difference between the dry and saturated adiabatic lapse rate. The average glacier mass balance used is −0.44 m y^{-1} with a standard deviation of 0.043 m y^{-1} (Sect. 3.4, Table 2). Based on these assumptions we sample 25 parameter sets and mass balance values. For each sampled parameter set and mass balance combination we recalibrate the CorT parameter. We then run a full simulation until 2050 with each of these 25 parameter combinations (i.e. of T_{lapse}, DDF_{CI}, DDF_{DC} and associated calibrated CorT) and we estimate uncertainty by taking the standard deviation of the 25 simulations (Ragettli and Pellicciotti, 2012). This analysis allows to estimate how a given uncertainty in parameters results in uncertainty in the glacier model simulations.

5 Results

To analyse differences in glacier extent projections for the CMIP3 and CMIP5 ensembles, we force the glacier model with the downscaled temperature and precipitation projections described in Sect. 4.1.

Figure 11, spanning the frequency space between the 10 and 90-percentiles for both temperature and precipitation, shows the percentual glacier retreat in 2050 for the

HESSD
9, 12691–12727, 2012

Uncertain future Central Asian glaciers

A. F. Lutz et al.

CMIP3 and the CMIP5 case. Both cases show large variability in future glacier extent. For the CMIP3 projections, a reduction in glacier area varying between 28 % in 2050 when the model is forced by the Q10 ΔT and the Q90 ΔP and a reduction of 55 % in 2050 when forced by the Q90 ΔT and Q10 ΔP is observed. By keeping ΔT constant at the Q50 level a 5 % uncertainty range in glacier extent retreat is found (from 42 % to 37 % decrease) over the full ΔP range for the CMIP3 case and a similar range is found when ΔP is kept constant. Although this uncertainty range is larger for the CMIP5 case (9 %) it is the same for precipitation and temperature. So, the uncertainty in precipitation projections has a similar impact on the uncertainty in glacier extent as uncertainty in temperature projections.

There are striking differences, however, between the results from the CMIP3 and CMIP5 based simulations. The CMIP5 models show greater warming and the median projection shows a decrease in glacier extent of 47 % compared to 43 % in the CMIP3 case. More important, the uncertainty range is wider. The Q10 ΔT and the Q90 ΔP combination results in a projected decrease of 29 %, while the Q90 ΔT and the Q10 ΔP combination leads to a decrease of 62 % (Fig. 11). The cold side of the distribution of changes is similar to CMIP3. However, the heavy tail in the distribution of temperature changes has a clear impact on the projections for the glacier extent and hints at the possibility that glaciers will retreat further than previously anticipated. Fig. 12 shows the spatial patterns of future glacier extent for 2050 for the AR5 median case and for the AR5 dry and warm case. Both maps reveal that the central Pamir shows the most persistent glacier extent, whereas in the Tien Shan and Alai ranges the glacier retreat is most prominent. This is mostly explained by the fact that the largest glacier systems are found in the central Pamir. The lower panels of Fig. 12 indicate that there is a considerable difference during the entire simulation period between CMIP3 and CMIP5 projections of glacier extent and that this difference is larger than the estimated error in the projections.

The estimated error in glacier extent in 2050 is ±4.4 % for the simulation with average temperature and precipitation change from the CMIP5 ensemble and ±4.1 % for the

HESSD
9, 12691–12727, 2012

CMIP3 ensemble respectively. The estimated uncertainty in 2050 glacier extent in the Q90 ΔT and the Q10 ΔP combination is ±5.0 % for the CMIP5 ensemble and ±4.6 % for the CMIP3 ensemble.

6 Discussion

To assess future changes in high mountain hydrology we rely on glacio-hydrological models. While mass balance modelling is rather straightforward to implement and approaches of different complexity can be used (from simple degree day to energy balance models for calculation of ablation), changes in glacier geometry due to ice flow are more complex to include in glacio-hydrological models. At the same time, changes in glacier geometry are important to include in regions where glacier melt makes a significant contribution to total runoff. Ideally, these should be simulated with mass balance models combined with two or three dimensional ice flow dynamics (Huss et al., 2007; Jouvet et al., 2008), but these are computationally demanding and require detailed knowledge of glacier velocities. Simpler approaches have been developed in which ice is transported from the accumulation zone to the ablation zone through basal sliding or creep (Immerzeel et al., 2011), but, like models of ice flow dynamics, this approach is only applicable for small catchments as it requires a high spatial resolution. A commonly used alternative method is to use area volume scaling relationships (Radić and Hock, 2011; van de Wal and Wild, 2001). Finally, in several hydrological models glaciers are treated as static entities that generate melt water and the glacier extent is modified for the future by making crude assumptions on the ice mass balance (Immerzeel et al., 2010) or by imposing hypothetical glacier scenarios (Finger et al., 2012; Rees and Collins, 2006; Singh and Bengtsson, 2004; Singh et al., 2006).

Parameterizations of future glacier evolution have been developed for individual glacier systems (Huss et al., 2010), but this approach requires time series of high resolution DEMs to assess past changes in ice volumes for calibration. This information is not routinely available, especially for large areas, making this approach less suitable for large river basins like in this study. Besides, it is not possible to model the dynamics of individual glaciers at the low spatial resolution used in large scale hydrological models. Several global scale models that simulate glacier mass balances have been developed (Hirabayashi et al., 2010; Radić and Hock, 2011). A gap exists between the global-scale and the catchment-scale models, and to our knowledge no suitable tools to assess glacier evolution at the large river basin scale are available.

Therefore, there is a strong need for an approach that can be applied at the large river basin scale, requires a minimum of data inputs which are readily available and which generalises glacier dynamics over large areas without the need to model individual glaciers. At the same time this approach has to yield a reliable estimate of future glacier extent at the large river basin scale. The model we developed and applied for this study simulates glacier evolution at high spatial resolution but with low data and computational demands, i.e. only initial glacierized area and regional averaged mass balance are required. Hence, it can be used to assess glacier evolution at the large river basin scale. The model is designed specifically for inclusion in large scale hydrological models under data scarce conditions, where glaciers need to be modelled at the sub-grid level as hydrological models at large scale usually have a spatial resolution that cannot resolve glaciological processes. The glacier model was developed for the Amu Darya and Syr Darya river basins in Central Asia, but can be applied in any (partly) glacierized basin.

The advantage of using the approach described in this paper of course comes with limitations. We use Bahr's volume-area scaling to estimate the initial ice volume based on the initial glacierized area and to translate new ice volumes to areas (Bahr et al., 1997). More accurate ways to estimate the initial ice volume are available (Farinotti et al., 2009; Paul and Linsbauer, 2012), however these methods require additional data besides glacier outlines which are often not readily available, as is the case in the studied basins.

In our model setup we construct one average hypsometric curve for the two river basins. This simplification constitutes a drawback as regional differences are

HESSD
9, 12691–12727, 2012

neglected. To retain more regional differences a more accurate glacier modelling could be done by constructing different hypsometric curves for different (sub)basins.

Another area for improvement is the melt modelling. We now use a combined degree day factor for debris free and debris covered glaciers. If the exact extent of both types of glaciers is available it would be recommendable to model both types separately. In addition, melt modelling under debris covered glaciers is not trivial and strong spatial variation is observed in the Alps as a result of the type and thickness of the debris layer and improved models for melt under debris should be used that account for the effect of debris thickness (Reid et al., 2012). These are all indications for future work. Despite the simplifications of the glacier model, however, which are dictated by the limited availability of glaciological data in the region, these should not affect our main result that differences within GCMs and between the two ensembles are strong and should be taken into account in impact studies.

7 Conclusions

Downstream water availability in several large Asian rivers is highly sensitive to changes in snow and glacier extent (Immerzeel et al., 2010). This dependence is likely to increase as irrigated areas further expand under population growth (Wada et al., 2011). Although both past and recent climate change projections point towards a decline of glacier extent, our results show that uncertainty about the size of this decline remains large. The range of projections for temperature and precipitation in the Central Asian region for the CMIP5 ensemble is larger than for the CMIP3 ensemble and the median projection for CMIP5 models shows greater warming than for CMIP3 models. Thus the CMIP5 ensemble leads to a wider range in projected glacier extent. Between the 10 and 90-percentiles for temperature and precipitation projections the median projection shows a decrease in glacier extent of 47 % for the CMIP5 ensemble compared to 43 % in the CMIP3 case. The projected decrease in glacier extent ranges from 29 % to 62 % for the CMIP5 ensemble compared to 28 % to 55 % for the CMIP3 ensemble.

HESSD
9, 12691–12727, 2012
Uncertain future Central Asian glaciers
A. F. Lutz et al.

This wide range demonstrates substantial uncertainty in climate change projections and associated glacier response for Central Asia. Furthermore it shows that it is imperative to use a representative selection of climate models and emission scenarios that span the entire range of possible future climates in climate change impact studies. The wide range in the projections implies an uncertain future, both in terms of Central Asian glacier extent as well as in terms of downstream water availability.

Acknowledgements. This work is part of the research program VENI, which is (partly) financed by the Netherlands Organization for Scientific Research (NWO). The updated GLIMS data set was provided by T. Bolch, University of Zurich, based on contributions by T. Khromova, N. Moelg and T. Bolch. This dataset will be made available soon through the GLIMS database (www.glims.org). Besides we thank M. Suklitsch, University of Graz, for the preparation of Fig. 3. We acknowledge the World Climate Research Program's Working Group on Coupled Modeling, which is responsible for CMIP, and we thank the climate modeling groups for producing and making available their model output. For CMIP the US. Department of Energy's Program for Climate Model Diagnosis and Intercomparison provides coordinating support and led development of software infrastructure in partnership with the Global Organization for Earth System Science Portals. We thank the World Glacier Monitoring Service for providing the regional glacier mass balance data.

References

Aizen, V. B., Aizen, E. M., and Kuzmichonok, V. A.: Glaciers and hydrological changes in the Tien Shan: simulation and prediction, Environ. Res. Lett., 2, 045019, 2007a.

Aizen, V. B., Kuzmichenok, V. A., Surazakov, A. B. and Aizen, E. M.: Glacier changes in the Tien Shan as determined from topographic and remotely sensed data, Global Planet. Change, 56, 328–340, 2007b.

Arnell, N. W.: Climate change and global water resources, Global Planet. Change, 9, S31–S49, 1999.

Bahr, D. B., Meier, M. F., and Peckham, S. D.: The physical basis of glacier volume-area scaling, J. Geophys. Res., 10, 20355–20362, 1997.

Bolch, T.: Climate change and glacier retreat in northern Tien Shan (Kazakhstan/Kyrgyzstan) using remote sensing data, Global Planet. Change, 56, 1–12, 2007.

Bolch, T., Kulkarni, A., Kääb, A., Huggel, C., Paul, F., Cogley, J. G., Frey, H., Kargel, J. S., Fujita, K., Scheel, M., Bajracharya, S., and Stoffel, M.: The State and Fate of Himalayan Glaciers, Science, 336, 310–314, 2012.

Cogley, J. G., Kargel, J. S., Kaser, G. and Van Der Veen, C. J.: Tracking the source of glacier misinformation, Science, 327, 522–522, 2010.

Danko, D. M.: The digital chart of the world project, Photogramm. Eng. Rem. S., 58, 1125–1128, 1992.

Deque, M.: Frequency of precipitation and temperature extremes over France in an anthropogenic scenario: Model results and statistical correction according to observed values, Global Planet. Change, 57, 16–26, 2007.

Farinotti, D., Huss, M., Bauder, A. and Funk, M.: An estimate of the glacier ice volume in the Swiss Alps, Global Planet. Change, 68(3), 225–231, 2009.

Finger, D., Heinrich, G., Gobiet, A. and Bauder, A.: Projections of future water resources and their uncertainty in a glacierized catchment in the Swiss Alps and the subsequent effects on hydropower production during the 21st century, Water Resour. Res., 48, 1–20, 2012.

Giesen, R. H. and Oerlemans, J.: Response of the ice cap Hardangerjøkulen in southern Norway to the 20th and 21st century climates, The Cryosphere, 4, 191–213, doi:10.5194/tc-4-191-2010, 2010.

Hagg, W., Mayer, C., Lambrecht, A. and Helm, A.: Sub-Debris Melt Rates on Southern Inylchek Glacier, Central Tian Shan, Geografiska Annaler, Series A: Physical Geography, 90, 55–63, 2008.

Hirabayashi, Y., Döll, P., and Kanae, S.: Global-scale modeling of glacier mass balances for water resources assessments: Glacier mass changes between 1948 and 2006, J. Hydrol., 390, 245–256, 2010.

Hsu, K. and Sorooshian, S.: Satellite-Based Precipitation Measurement Using PERSIANN System, in: Hydrological Modelling and the Water Cycle, 27–48, 2009.

Huss, M.: Present and future contribution of glacier storage change to runoff from macroscale drainage basins in Europe, Water Resour. Res., 47, W07511, 2011.

Huss, M., Jouvet, G., Farinotti, D., and Bauder, A.: Future high-mountain hydrology: a new parameterization of glacier retreat, Hydrol. Earth Syst. Sci., 14, 815–829, doi:10.5194/hess-14-815-2010, 2010.

Huss, M., Sugiyama, S., Bauder, A. and Funk, M.: Retreat Scenarios of Unteraargletscher, Switzerland, Using a Combined Ice-Flow Mass-Balance Model, Water Resour., 39, 422–431, 2007.

Immerzeel, W. W., Van Beek, L. P. H., and Bierkens, M. F. P.: Climate change will affect the Asian water towers., Science, 328, 1382–5, 2010.

Immerzeel, W. W., van Beek, L. P. H., Konz, M., Shrestha, A. B., and Bierkens, M. F. P.: Hydrological response to climate change in a glacierized catchment in the Himalayas, Climatic Change, 110, 721–736, 2011.

Immerzeel, W. W., Lutz, A. F., and Droogers, P.: Climate Change Impacts on the Upstream Water Resources of the Amu and Syr Darya River Basins, Wageningen, The Netherlands, 103 pp., 2012.

Immerzeel, W. W., Pellicciotti, F., and Shrestha, A. B.: Glaciers as a Proxy to Quantify the Spatial Distribution of Precipitation in the Hunza Basin, Mt. Res. Dev., 32, 30–38, 2012b.

Jouvet, G., Picasso, M., Rappaz, J., and Blatter, H.: A new algorithm to simulate the dynamics of a glacier: theory and applications, J. Glaciol., 54, 801–811, 2008.

Kargel, J. S., Cogley, J. G., Leonard, G. J., Haritashya, U., and Byers, A.: Himalayan glaciers: The big picture is a montage, P. Natl. Acad. Sci. USA, 108, 14709–14710, 2011.

Kaser, G., Großhauser, M., and Marzeion, B.: Contribution potential of glaciers to water availability in different climate regimes., P. Natl. Acad. Sci. USA, 2010, 1–5, 2010.

Kaushik, G., Wang, N.-Y., Ferraro, R., and Liu, C.: Status of the TRMM 2A12 Land Precipitation Algorithm, J. Atmos. Ocean. Tech., 27, 1343–1354, 2010.

Kay, A. L., Davies, H. N., Bell, V. A., and Jones, R. G.: Comparison of uncertainty sources for climate change impacts: flood frequency in England, Climatic Change, 92, 41–63, 2008.

Khromova, T. E., Dyurgerov, M. B., and Barry, R. G.: Late-twentieth century changes in glacier extent in the Ak-shirak Range, Central Asia, determined from historical data and ASTER imagery, Geophys. Res. Lett., 30, 3–7, 2003.

Khromova, T. E., Osipova, G. B., Tsvetkov, D. G., Dyurgerov, M. B. and Barry, R. G.: Changes in glacier extent in the eastern Pamir, Central Asia, determined from historical data and ASTER imagery, Remote Sens. Environ., 102, 24–32, 2006.

Meehl, G. A., Covey, C., Delworth, T., Latif, M., Mcavaney, B., Mitchell, J. F. B., Stouffer, R. J., and Taylor, K. E.: The WCRP CMIP3 multimodel dataset: A New Era in Climate Change Research, B. Am. Meteorol. Soc., (September), 1382–1394, 2007.

HESSD

9, 12691–12727, 2012

Uncertain future Central Asian glaciers

A. F. Lutz et al.

Meinshausen, M., Smith, S. J., Calvin, K., Daniel, J. S., Kainuma, M. L. T., Lamarque, J.-F., Matsumoto, K., Montzka, S. A., Raper, S. C. B., Riahi, K., Thomson, A., Velders, G. J. M., and Vuuren, D. P. P.: The RCP greenhouse gas concentrations and their extensions from 1765 to 2300, Climatic Change, 109(1), 213–241, 2011.

Menon, S., Koch, D., Beig, G., Sahu, S., Fasullo, J., and Orlikowski, D.: Black carbon aerosols and the third polar ice cap, Atmos. Chem. Phys., 10, 4559–4571, doi:10.5194/acp-10-4559-2010, 2010.

Mihalcea, C., Mayer, C., Diolaiuti, G., Lambrecht, A., Smiraglia, C., and Tartari, G.: Ice ablation and meteorological conditions on the debris-covered area of Baltoro glacier, Karakoram, Pakistan, Ann. Glaciol., (1894), 292–300, 2006.

Nakicenovic, N., Alcamo, J., Davis, G., de Vries, B., Fenhann, J., Gaffin, S., Gregory, K., Grubler, A., Jung, T. Y., Kram, T., La Rovere, E. L., Michaelis, L., Mori, S., Morita, T., Pepper, W., Pitcher, H. M., Price, L., Riahi, K., Roehrl, A., Rogner, H.-H., Sankovski, A., Schlesinger, M., Shukla, P., Smith, S. J., Swart, R., van Rooijen, S., Victor, N., and Dadi, Z.: Special Report on Emissions Scenarios: A Special Report of Working Group III of the Intergovernmental Panel on Climate Change, Cambridge, UK, 2000.

Narama, C., Kääb, A., Duishonakunov, M. and Abdrakhmatov, K.: Spatial variability of recent glacier area changes in the Tien Shan Mountains, Central Asia, using Corona (∼1970), Landsat (∼2000), and ALOS (∼2007) satellite data, Global Planet. Change, 71, 42–54, 2010.

Paul, F. and Linsbauer, A.: Modeling of glacier bed topography from glacier outlines, central branch lines, and a DEM, Int. J. Geogr. Inf. Sci., 26, 1–18, 2012.

Radić, V., and Clarke, G. K. C.: Evaluation of IPCC Models' Performance in Simulating Late-Twentieth-Century Climatologies and Weather Patterns over North America, J. Climate, 24, 5257–5274, 2011.

Radić, V. and Hock, R.: Regionally differentiated contribution of mountain glaciers and ice caps to future sea-level rise, Nat. Geosci., 4, 91–94, 2011.

Ragettli, S. and Pellicciotti, F.: Calibration of a physically based, spatially distributed hydrological model in a glacierized basin: On the use of knowledge from glaciometeorological processes to constrain model parameters, Water Resour. Res., 48, W03509, 2012.

Raup, B., Kaab, a, Kargel, J., Bishop, M., Hamilton, G., Lee, E., Paul, F., Rau, F., Soltesz, D., and Khalsa, S.: Remote sensing and GIS technology in the Global Land Ice Measurements from Space (GLIMS) Project, Comput. Geosci., 33, 104–125, 2007.

HESSD

9, 12691–12727, 2012

Uncertain future Central Asian glaciers

A. F. Lutz et al.

Rees, H. G. and Collins, D. N.: Regional differences in response of flow in glacier-fed Himalayan rivers to climatic warming, Hydrol. Process., 20, 2157–2169, 2006.
Reid, T. D., Carenzo, M., Pellicciotti, F., and Brock, B. W.: Including debris cover effects in a distributed model of glacier ablation, J. Geophys. Res., 117, D18105, 2012.
Siegfried, T., Bernauer, T., Guiennet, R., Sellars, S., Robertson, A. W., Mankin, J., Bauer-Gottwein, P., and Yakovlev, A.: Will climate change exacerbate water stress in Central Asia?, Climatic Change, 112, 881–899, 2012.
Singh, P. and Bengtsson, L.: Hydrological sensitivity of a large Himalayan basin to climate change, Hydrol. Process., 18, 2363–2385, 2004.
Singh, P., Arora, M., and Goel, N. K.: Effect of climate change on runoff of a glacierized Himalayan basin, Hydrol. Process., 20, 1979–1992, 2006.
Sorg, A., Bolch, T., Stoffel, M., Solomina, O. and Beniston, M.: Climate change impacts on glaciers and runoff in Tien Shan (Central Asia), Nature Climate Change, 2, 725–731, 2012.
Taylor, K. E., Stouffer, R. J., and Meehl, G. A.: An Overview of CMIP5 and the Experiment Design, B. Am. Meteorol. Soc., 93, 485–498, 2012.
Wada, Y., van Beek, L. P. H., and Bierkens, M. F. P.: Modelling global water stress of the recent past: on the relative importance of trends in water demand and climate variability, Hydrol. Earth Syst. Sci., 15, 3785–3808, doi:10.5194/hess-15-3785-2011, 2011.
van de Wal, R. S. W. and Wild, M.: Modelling the response of glaciers to climate change by applying volume-area scaling in combination with a high resolution GCM, Clim. Dynam., 18, 359–366, 2001.
WGMS: Glacier Mass Balance Bulletin No. 11 (2008–2009). Zemp, M., Nussbaumer, S. U., Gärtner-Roer, I., Hoelzle, M., Paul, F., and Haeberli, W. (eds.), ICSU(WDS)/IUGG(IACS)/UNEP/UNESCO/WMO, World Glacier Monitoring Service, Zurich, Switzerland, 2011.
Zhang, Y., Liu, S., and Ding, Y.: Observed degree-day factors and their spatial variation on glaciers in western China, Ann. Glaciol., 43, 301–306, 2006.

HESSD
9, 12691–12727, 2012

Uncertain future Central Asian glaciers

A. F. Lutz et al.

Title Page
Abstract | Introduction
Conclusions | References
Tables | Figures
◀| |▶
◀ ▶
Back | Close
Full Screen / Esc
Printer-friendly Version
Interactive Discussion

Table 1. Model parameters used in the glacier model. T_{lapse} and CorT were calibrated in this study, DDF_{CI} and DDF_{DC} were calibrated in a related hydrological study (Immerzeel et al., 2012a), MB_{obs} is taken from (WGMS, 2011).

Parameter	Parameter description	Value
T_{lapse}	Temperature lapse rate	–0.0068 °C m^{-1}
DDF_{CI}	Degree day factor debris free glaciers	7.95 mm °C^{-1} day^{-1}
DDF_{DC}	Degree day factor debris covered glaciers	3.97 mm °C^{-1} day^{-1}
CorT	Correction temperature	2.59 °C
MB_{obs}	Observed mass balance, (WGMS, 2011), see Table 2	–0.44 m w.e. year^{-1}

HESSD
9, 12691–12727, 2012

Table 2. Observed mass balance data since 1991 for several bench mark glaciers (WGMS, 2011).

Glacier name	Mountain range	Latitude (decimal degrees)	Longitude (decimal degrees)	Mass balance (mm w.e. y^{-1}) (1991–2010)
Abramov	Pamir – Alai	39.63	71.60	–393
Golubin	Tien Shan	42.47	74.50	–451
Kara Batkak	Tien Shan	42.10	78.30	–417
Tuyuksuyskiy	Tien Shan	43.05	77.08	–432
Urumqi	Tien Shan	43.08	86.82	–507
Average				–440
Standard deviation				43

HESSD
9, 12691–12727, 2012

Title Page
Abstract Introduction
Conclusions References
Tables Figures
◀ ▶
Back Close
Full Screen / Esc
Printer-friendly Version
Interactive Discussion

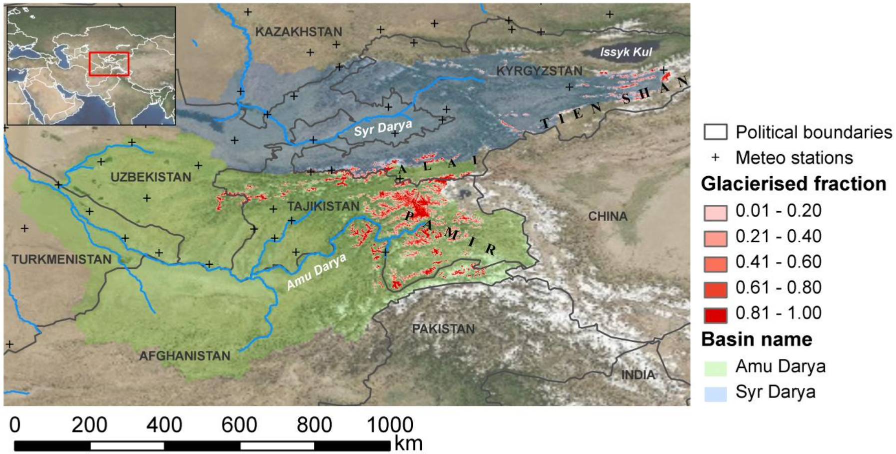

Fig. 1. Upstream parts of the Amu and Syr Darya river basins (in green and pale blue, respectively), the main river system (blue lines), the present day glacierized fraction per 1 km grid cell (red shades), political boundaries (black lines), and meteorological stations (black crosses).

HESSD
9, 12691–12727, 2012

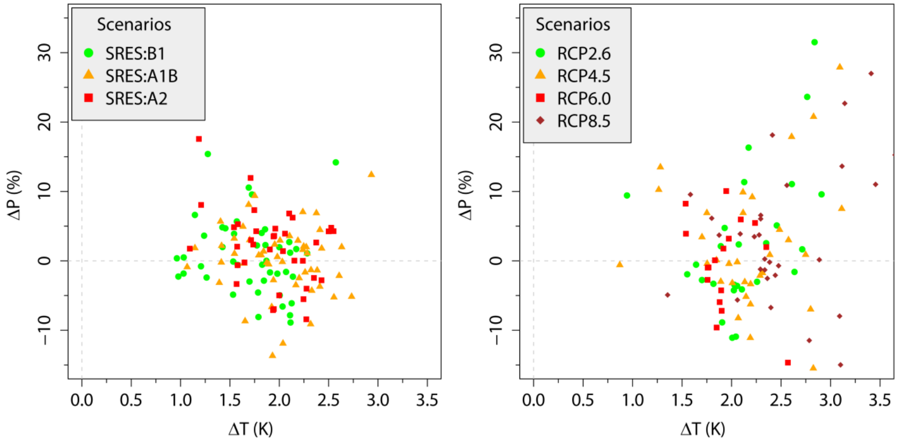

Fig. 2. Complete range of projected changes (2021-2050 relative to 1961-1990) in temperature and precipitation in the upstream areas of the Amu and Syr Darya river basins. The left panel shows model runs used for the fourth assessment report of the IPCC (AR4) for three different emission scenarios (A1B (53 runs), A2 (36 runs), B1 (44 runs)). The right panel shows model runs that will be used for the fifth assessment report (AR5, all simulations available before 15 December 2011 are included) for four representative concentration pathways (RCP2.6 (26 runs), RCP4.5 (32 runs), RCP6.0 (17 runs), RCP8.5 (29 runs)).

HESSD
9, 12691–12727, 2012

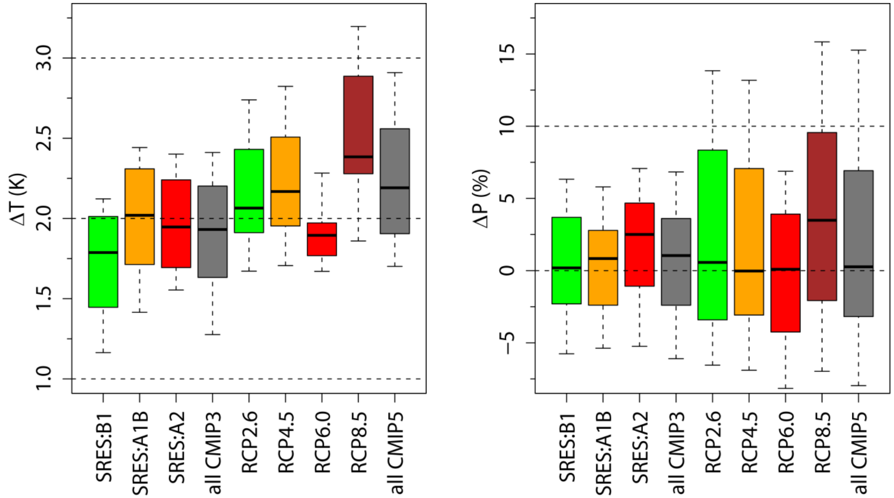

Fig. 3. Box-whisker plots for projected changes in temperature (left) and precipitation (right) for three AR4 SRES emission scenarios and four AR5 representative concentration pathways extracted from the CMIP3 (SRES) and CMIP5 (RCP) databases. The A1B (53 GCM runs), A2 (36 runs) and B1 (44 runs) AR4 scenarios are used and the RCP2.6 (26 runs), RCP4.5 (32 runs), RCP6.0 (17 runs) and RCP8.5 (29 runs) AR5 scenarios are used.

HESSD

9, 12691–12727, 2012

Uncertain future Central Asian glaciers

A. F. Lutz et al.

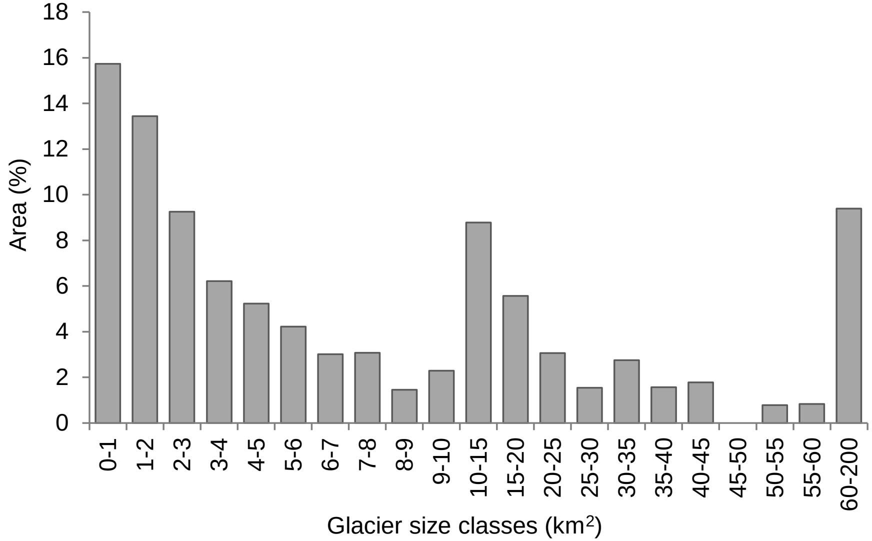

Fig. 4. Distribution of glacier area over glacier size classes for the two basins combined.

HESSD

9, 12691–12727, 2012

Uncertain future Central Asian glaciers

A. F. Lutz et al.

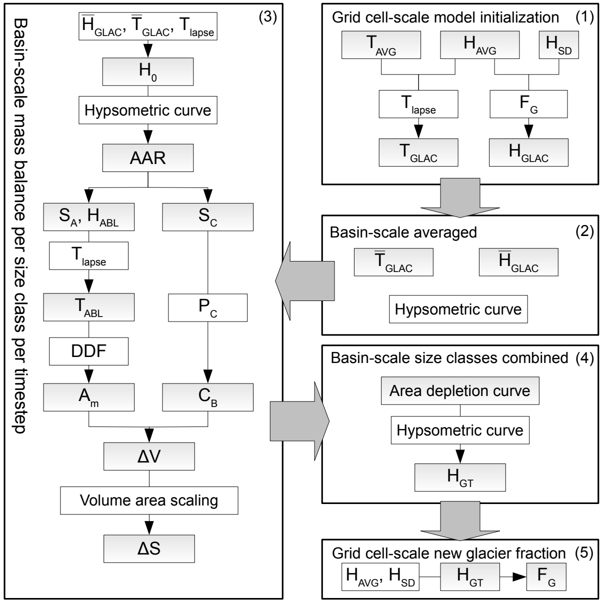

Fig. 5. Schematic representation of glacier modelling steps. The model is initialized at the 1 km grid cell scale (1). The results of step 1 are combined to construct a basin-scale hypsometric curve and basin-scale averaged T_{GLAC} and H_{GLAC} (2). Basin-scale mass balance calculations are done for 21 glacier size classes with a monthly time step (3). With result from step 3 a basin-scale area depletion curve is constructed to calculate H_{GT} for each time step (4). With H_{GT} and the elevation distribution within a grid cell, the basin-scale model output is downscaled to the grid-cell scale for each time step (5).

HESSD
9, 12691–12727, 2012

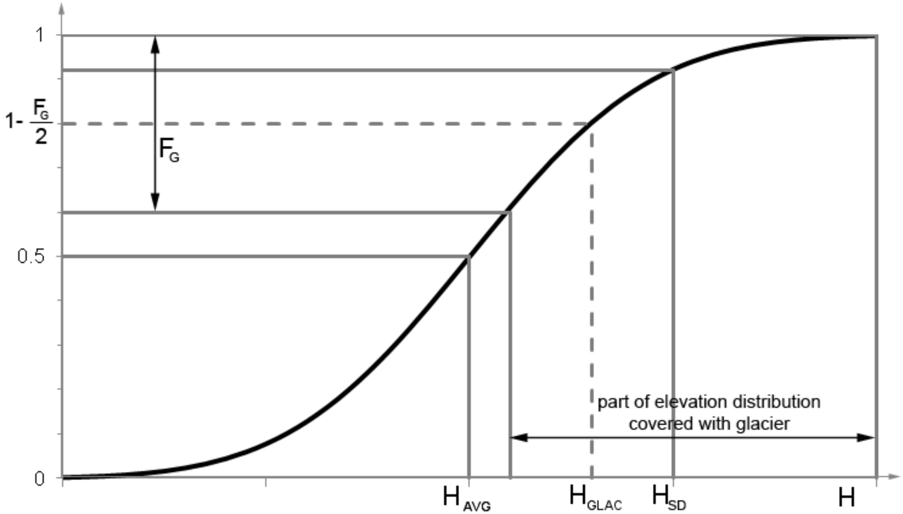

Fig. 6. Distribution of elevation within a 1 km grid cell. H_{AVG} is the mean elevation in a 1 km grid cell. H_{SD} is the standard deviation of the elevation distribution. F_G is the fractional glacier cover for a 1 km grid cell. H_{GLAC} is the obtained representative elevation for the part of the grid cell covered with glaciers. In this figure $F_G = 0.4$.

HESSD
9, 12691–12727, 2012

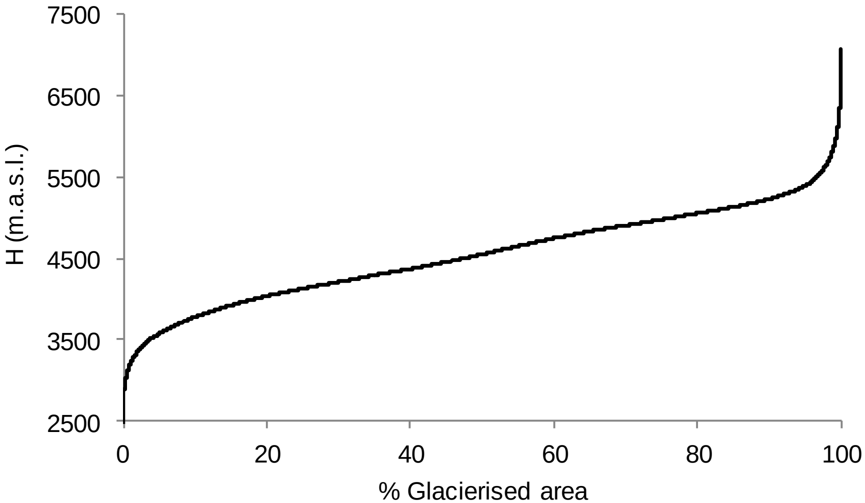

Fig. 7. Basin scale hypsometric curve for elevation (H) and glacierized area for both basins.

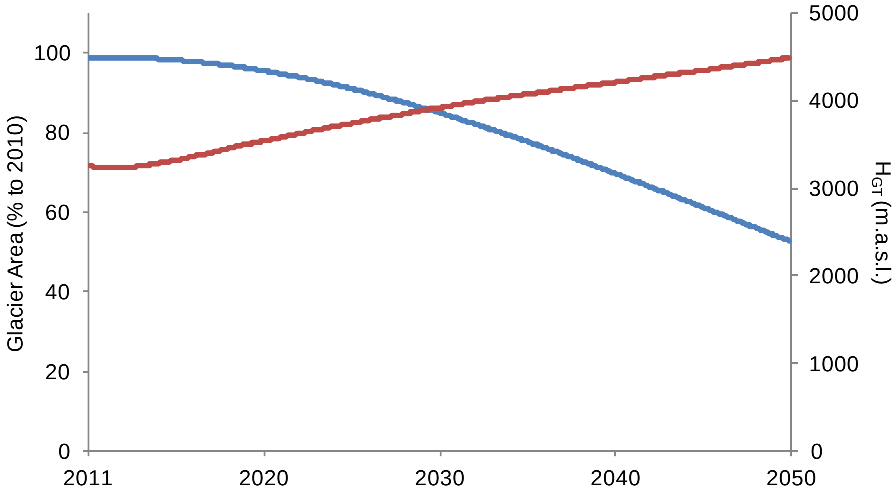

Fig. 8. Relative change in glacier area aggregated for all size classes (blue line) and threshold elevation for glaciers to persist (H_{GT}) (red line).

HESSD
9, 12691–12727, 2012

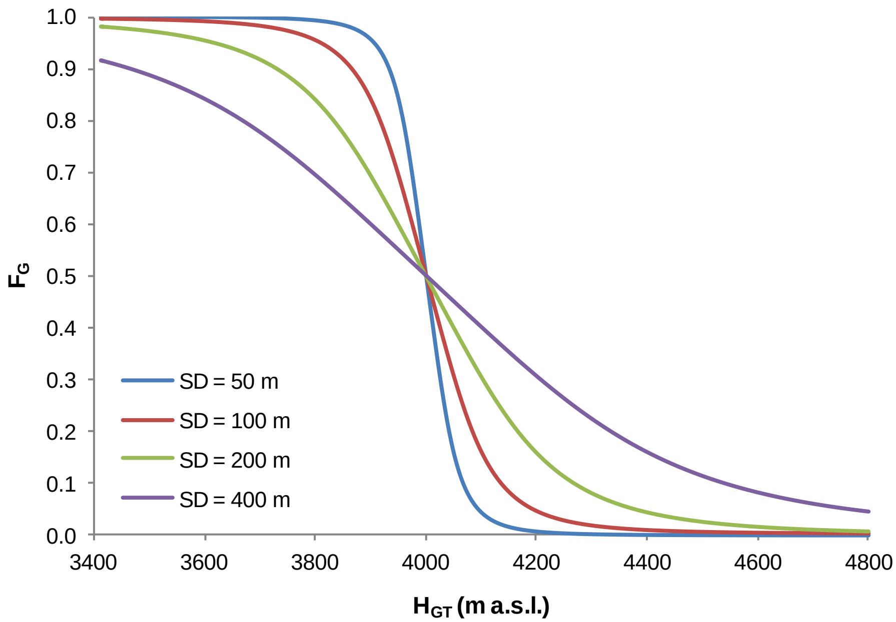

Fig. 9. Fractional glacier coverage (F_G) as function of glacier threshold elevation (H_{GT}) for a 1 × 1 km grid cell with 4000 m average elevation and variable standard deviation (SD).

HESSD
9, 12691–12727, 2012

Uncertain future Central Asian glaciers

A. F. Lutz et al.

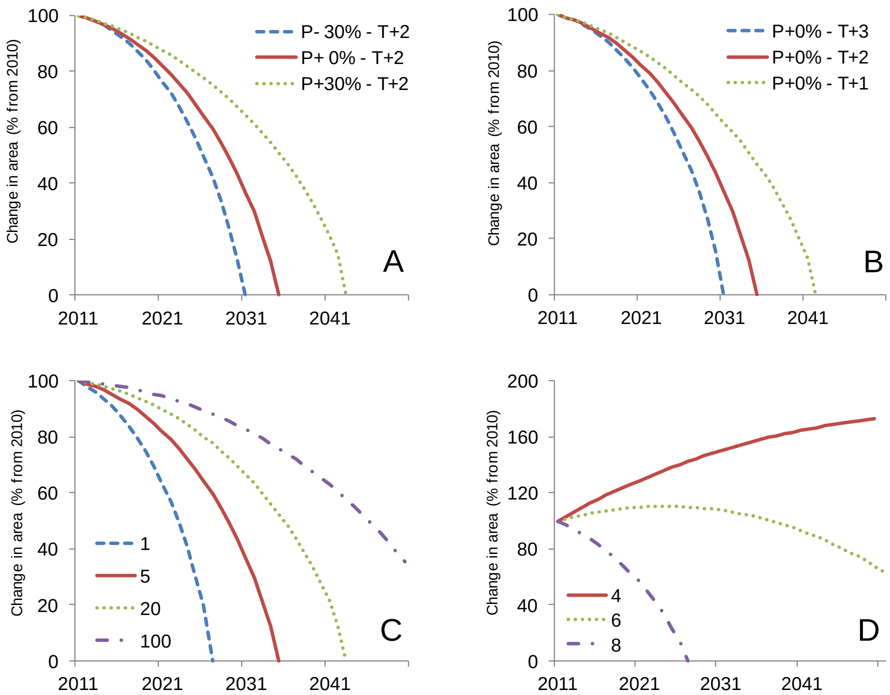

Fig. 10. Hypothetical future glacier evolution as a function of precipitation **(A)**, temperature **(B)**, glacier size **(C)** and melt properties **(D)**. Baseline properties are: a glacier with a size of 5 km^2 and a projected temperature increase of 2°C in 2050 relative to 2001 – 2010 and no precipitation change. All changes are ceteris paribus. Panel A shows the sensitivity to a precipitation change (–30 %, 0 %, +30 %) in 2050. Panel B shows the sensitivity to a temperature change of 1 °C, 2 °C and 3 °C in 2050. Panel C shows the effect of glacier size for a 1 km^2, 5 km^2, 20 km^2 and 100 km^2 on change in glacier extent in 2050. Panel D shows the effect of melt rate on change in glacier extent in 2050 assuming a degree day factor of 4 mm °C day^{-1}, 6 mm °C day^{-1} and 8 mm °C day^{-1}.

HESSD
9, 12691–12727, 2012

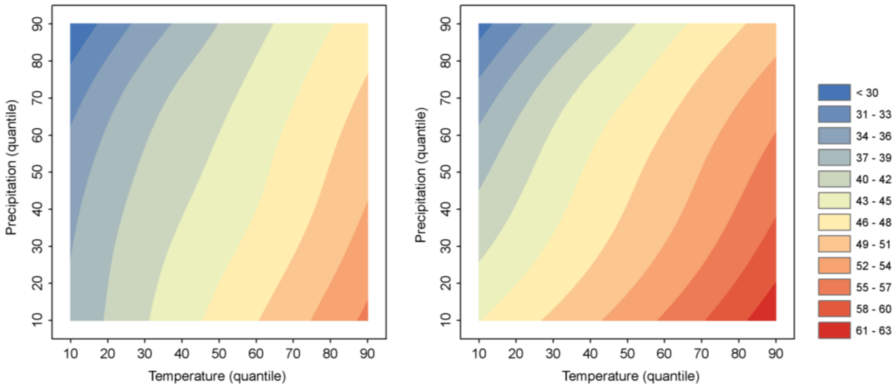

Fig. 11. Decrease in glacierized area in 2050 (% decrease relative to 2010) for the upstream parts of the Amu Darya and Syr Darya river basins for the changes in temperature and precipitation for CMIP3 runs (left) and CMIP5 runs (right).

HESSD
9, 12691–12727, 2012

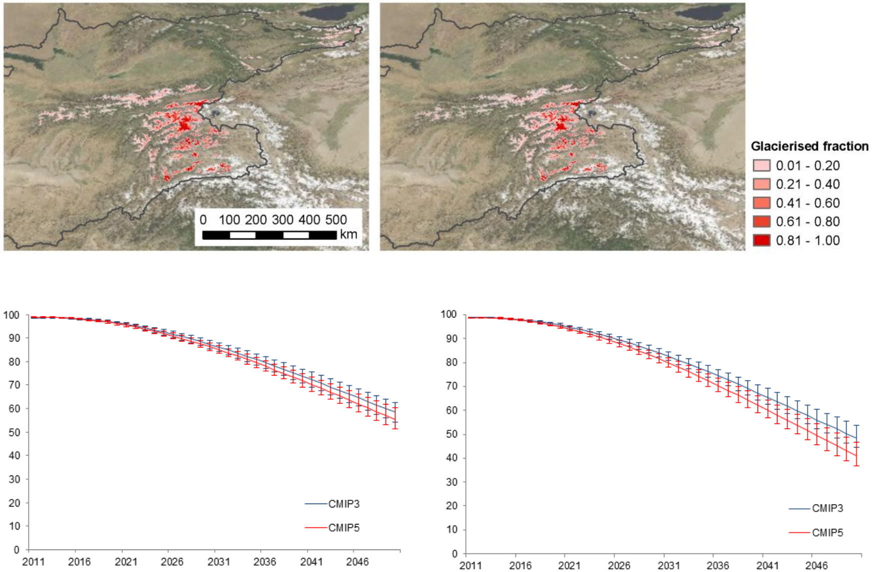

Fig. 12. Glacier extent in 2050 based on the CMIP5 model runs for the 50th percentile (Q50) values of precipitation and temperature change (top left) and for the dry (Q10) and warm (Q90) case (top right). The bottom panels show the decrease in glacier area with time for the CMIP3 and CMIP5 runs. The left figure show the Q50 case for both precipitation and temperature. The right figure shows the Q10 case for precipitation and the Q90 case for temperature. The error bars are derived using a uncertainty analysis on critical model parameters and observed glacier mass balance information (see Sect. 4.3).